Age and Rate of Accumulation of Metal-Rich Hydrothermal Deposits on the Seafloor: The Lucky Strike Vent Field, Mid-Atlantic Ridge

Dennis Sánchez-Mora, John Jamieson, Mathilde Cannat, Javier Escartín, Thibaut Barreyre

JGR Solid Earth

RESEARCH ARTICLE
10.1029/2022JB024031

Age and Rate of Accumulation of Metal-Rich Hydrothermal Deposits on the Seafloor: The Lucky Strike Vent Field, Mid-Atlantic Ridge

Dennis Sánchez-Mora[1], John Jamieson[1], Mathilde Cannat[2], Javier Escartín[3], and Thibaut Barreyre[4]

[1]Department of Earth Sciences, Memorial University of Newfoundland, St. John's, Newfoundland and Labrador, Canada, [2]Université de Paris, Institut de Physique du Globe de Paris, UMR CNRS, Paris, France, [3]Laboratoire de Géologie – CNRS, PSL University, Paris, France, [4]Department of Earth Science/Centre for Deep Sea Research, University of Bergen, Bergen, Norway

Key Points:

- Hydrothermal activity at the Lucky Strike vent field has been ongoing for at least 6,600 years
- An estimated ~1.3 Mt of hydrothermal material has accumulated on the seafloor over an area of <2.5 km^2 of seafloor, at a rate of ~194 t/yr
- Accumulation rates from Lucky Strike are comparable to other seafloor sites and to analogous on-land volcanogenic massive sulfide deposits

Supporting Information:

Supporting Information may be found in the online version of this article.

Correspondence to:

D. Sánchez-Mora,
dsanchezmora@mun.ca

Citation:

Sánchez-Mora, D., Jamieson, J., Cannat, M., Escartín, J., & Barreyre, T. (2022). Age and rate of accumulation of metal-rich hydrothermal deposits on the seafloor: The Lucky Strike vent field, Mid-Atlantic Ridge. *Journal of Geophysical Research: Solid Earth*, *127*, e2022JB024031. https://doi.org/10.1029/2022JB024031

Received 26 JAN 2022
Accepted 15 MAY 2022

Author Contributions:

Conceptualization: Dennis Sánchez-Mora, John Jamieson
Data curation: Dennis Sánchez-Mora, Mathilde Cannat, Thibaut Barreyre
Funding acquisition: John Jamieson
Methodology: Dennis Sánchez-Mora
Resources: Mathilde Cannat
Supervision: John Jamieson
Writing – original draft: Dennis Sánchez-Mora
Writing – review & editing: John Jamieson, Mathilde Cannat, Thibaut Barreyre

Abstract Hydrothermal venting at the Lucky Strike hydrothermal field, located on the Mid-Atlantic Ridge, is associated with faulting linked to the tectonic dismemberment of a central axial volcano. Radium-226/Ba dating of hydrothermal barite indicates that hydrothermal venting is at least 6,600 years old, and that Lucky Strike is one of the youngest known vent fields on the Mid-Atlantic Ridge, which typically have ages exceeding 20 ka. Deposit volume calculations indicate that the total accumulated mass of the hydrothermal deposits on the seafloor at Lucky Strike is ~1.3 ± 0.2 Mt, and that this mass accumulated at a maximum average rate of 194 ± 28 t/yr. This accumulation rate is comparable to other well characterized mid-ocean ridge hydrothermal sites, such as TAG and Endeavor, but at Lucky Strike is concentrated within a relatively small area of <2.5 km^2.

Plain Language Summary In this contribution we determine the age (>6,600 years) and mass (~1.3 Mt) of metal-rich deposits that formed at a cluster of high-temperature seafloor hot springs called Lucky Strike, which is situated on the Mid-Atlantic Ridge. With this information we calculate the average rate of formation (194 t/yr) of these deposits. Our results indicate that the Lucky Strike vent field is much younger than other vent fields that also occur along the Mid-Atlantic Ridge, but the deposits form at similar rates, which are high when compared to other types of geological processes that produce metal-rich deposits.

1. Introduction

Hydrothermal deposits form at and below the ocean floor due to subseafloor hydrothermal circulation associated with magmatism and faulting (Hannington, 2014, and references therein; Lowell et al., 1995). The ages of these deposits provide insights into the longevity and history of hydrothermal venting and rates at which these deposits form (Jamieson et al., 2014; Lalou et al., 1990). Several hydrothermal sites on volcanic arcs (e.g., de Ronde et al., 2005; Ditchburn et al., 2012) and mid-ocean ridges (MORs) (e.g., Cherkashov et al., 2017; Jamieson et al., 2013; Lalou & Brichet, 1982; Lalou et al., 1990; Münch et al., 2001; Wang et al., 2012) have been dated using U-series dating techniques. Vent fluid flux, temperatures, and compositions can be used to estimate chemical mass fluxes and deposit growth rates at time scales applicable to human observations (e.g., ranging from direct observation and sampling over seconds to minutes to repeat sampling and observations over years or decades; Barreyre et al., 2012; Lowell et al., 1995; Mittelstaedt et al., 2012, and references therein). However, to determine average rates of accumulation over the lifespan of a vent field, accurate estimates of deposit size are also required, together with age constraints. We define accumulation rate here as the total amount of hydrothermal deposition on the seafloor (measured as volume and converted to mass using estimated average density) relative to the oldest age determined for the site. This is therefore an average rate and does not consider that instantaneous rates may be variable over the lifespan of the hydrothermal system (Lalou et al., 1990), nor does it consider subseafloor deposition.

Of the seafloor hydrothermal deposits that have been dated thus far, only the Endeavor and TAG vent fields have been mapped at a high enough resolution to accurately determine the amount of hydrothermal material deposited on the seafloor (Graber et al., 2020; Jamieson et al., 2014). At Endeavor, 1.2 Mt of hydrothermal sulfide/sulfate/silica material accumulated over ~3,000 years, at an average rate of 400 t/yr (Jamieson et al., 2014). At TAG, 29 Mt of material accumulated over 100,000 years at an average rate of 300 t/yr (Graber et al., 2020). However,

at TAG, the dating work by Lalou et al. (1990) suggests that active venting occurred over only 20,000 years of the 100,000 years lifespan of the field, indicating that average accumulation rates during discontinuous periods of activity may be as high as 1,500 t/yr.

The Lucky Strike hydrothermal vent field, located on the Mid-Atlantic Ridge (MAR), is situated on an active axial volcano and is therefore considered to be young, relative to TAG and other MAR-hosted hydrothermal vent fields, which have ages of up to 230 ka (Cherkashov et al., 2017). In this study, we use a similar approach to Jamieson et al. (2014), and report results from ^{226}Ra/Ba dating of hydrothermal barite at Lucky Strike to constrain the history and evolution of the vent field, and mass accumulation rates. We couple these results with deposit tonnage estimates derived from high-resolution (~1 m) bathymetric data to determine the rates of deposit formation. The results of this study provide insights into formation rates for ancient volcanogenic massive sulfide (VMS) deposits.

2. Geological Setting

The Lucky Strike segment hosts a prominent axial volcano, named the Lucky Strike Seamount, that rises up from the central part of the segment. Recent episodes of volcanism produced two volcanic edifices that are aligned along the ridge axis, and which are separated by a flat depression that is interpreted to be a remnant fossil lava lake (Figure 1a; Humphris et al., 2002; Ondréas et al., 2009). Both volcanic edifices are now cut by a series of ridge-parallel normal faults, with the older, northern, volcanic edifice exhibiting a higher degree of rifting than the younger, southern, volcanic edifice (Humphris et al., 2002). The remains of the fossil lava lake overprint, and are therefore younger than the faults (Figure 1a).

Hydrothermal materials were first recovered in 1992 via dredging (Langmuir et al., 1992), and mounds and chimneys were located in 1993 using HOV Alvin (Langmuir et al., 1997). This was followed by additional dives in 1994 using HOV Nautile, and by autonomous underwater vehicle (AUV) and remotely operated vehicle (ROV) bathymetric mapping coupled with photomosaic imaging (Figures 1b and 1c; Barreyre et al., 2012; Fouquet et al., 1995; Langmuir et al., 1997; Ondréas et al., 2009). Hydrothermal venting occurs predominantly around the edges of the fossil lava lake, in clusters such as Sintra, Tour Eiffel, Y3, and others (Figures 1 and 2). Venting is interpreted to be genetically associated with an underlying axial magma chamber and is spatially associated with the most recent episode of faulting (Singh et al., 2006). Two other isolated hydrothermal vents occur outside of the main vent field; Capelinhos is located 1.4 km east of the central rift axis while Ewan occurs 1.5 km south of the main field (Figure 1a; Escartín et al., 2015). The spatial association of hydrothermal vents and fault traces, observed both within the main Lucky Strike field and at the Capelinhos vent site, suggests that faulting is a primary control on subseafloor fluid channeling, although fluids are likely redistributed where faults intersect the fossil lava lake (Barreyre et al., 2012; Escartín et al., 2015; Humphris et al., 2002).

The deposits at Lucky Strike are composed of a sulfide-sulfate mineral assemblage that is typical of hydrothermal deposits on the MAR (e.g., Bogdanov et al., 2006; Langmuir et al., 1997), with the notable exception of abundant barite, which has been linked to the enriched MOR basalt substrate associated with the Azores hotspot (Langmuir et al., 1997). There are two main modes of deposition of hydrothermal material on the seafloor at Lucky Strike; hydrothermally cemented volcaniclastic breccias; and massive sulfide-sulfate mounds and chimneys (Figure 3). The occurrence of barite allows for the hydrothermal deposits to be dated using the ^{226}Ra/Ba dating method (de Ronde et al., 2005; Ditchburn & de Ronde, 2017; Ditchburn et al., 2004, 2012).

3. Methodology

3.1. ^{226}Ra/Ba Dating

Rock samples for this study were collected from hydrothermal vents using the ROV *Victor 6000* during the Momarsat campaigns from 2011 to 2015 while on the R/V *Pourquoi pas ?* and R/V Thalassa (2012). Seventeen barite-rich samples were dated using the ^{226}Ra/Ba method (Ditchburn & de Ronde, 2017; Ditchburn et al., 2004, 2012; Jamieson et al., 2013). Ages are calculated by determining the amount of ^{226}Ra within barite that has decayed since formation:

$$t = \frac{\ln\left(N_0/N\right) \times 1600\,\text{years}}{\ln 2}$$

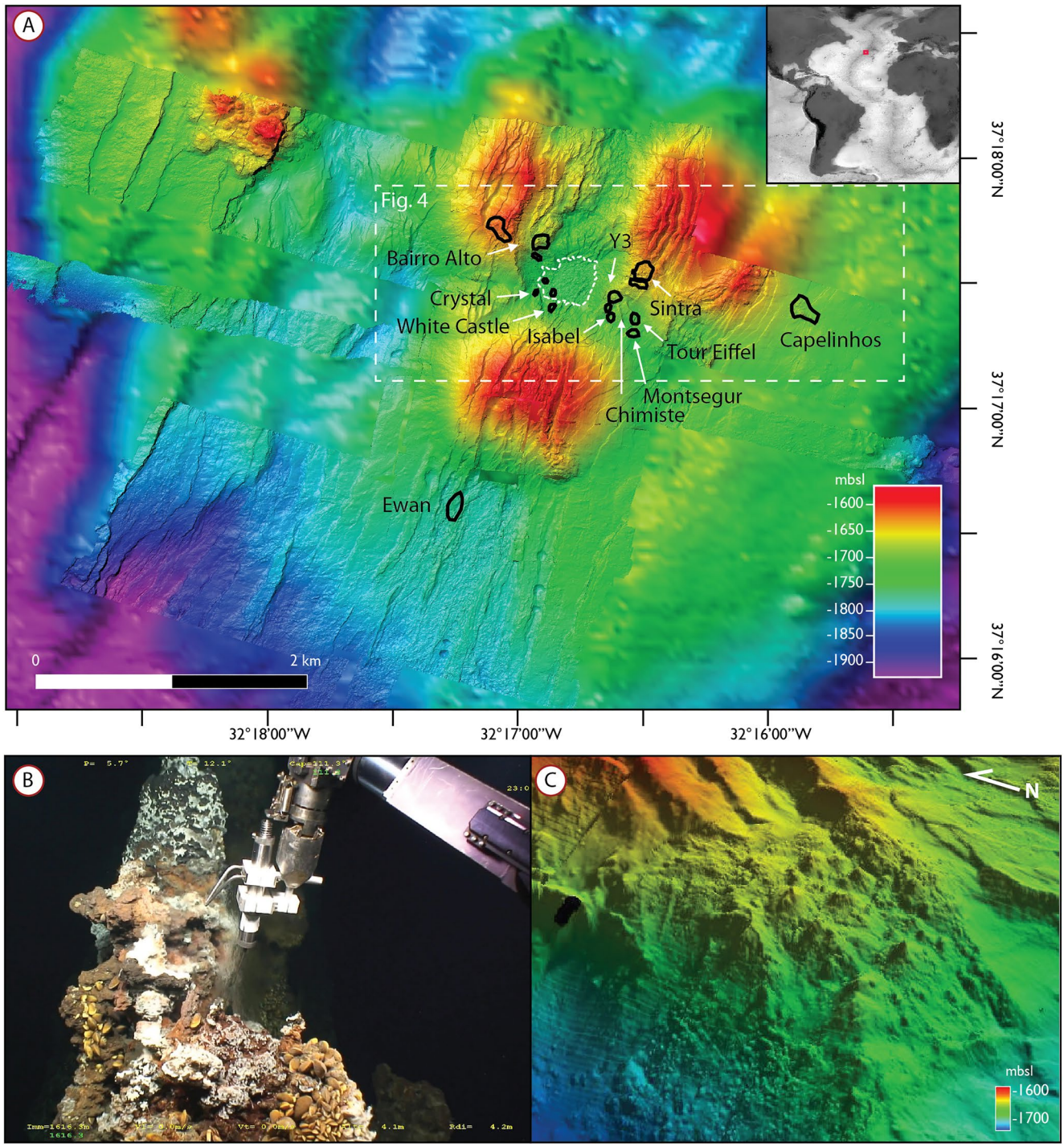

Figure 1. (a) Bathymetric map with outlines (solid black lines) of hydrothermal deposits at Lucky Strike. The white irregular dashed outline shows the extent of a solidified recent fossil lava lake. High temperature venting (>200°C) occurs within the main vent cluster that surrounds the fossil lava lake, and at Capelinhos. Ewan is a site of diffuse fluid flow. (b) Venting of up to 222°C (Charlou et al., 2000) at a sulfide chimney at the Sintra vent complex. (c) High-resolution (~1 m) bathymetry shows hydrothermal mounds and chimneys at the Sintra site. Bathymetry sources (Escartín et al., 2015, 2021; Ondréas et al., 2009).

where t = time (years), N_0 = initial ^{226}Ra/Ba of the sample at the time of crystallization, N = the measured ^{226}Ra/Ba of the sample, and 1,600 years the half-life of ^{226}Ra. The ^{226}Ra/Ba method relies on the assumption that the initial ^{226}Ra/Ba does not vary significantly over the period of venting (de Ronde et al., 2005). The lower age limit for the ^{226}Ra/Ba dating technique is ~500 years old (Ditchburn et al., 2004, 2012). To determine N_0, two

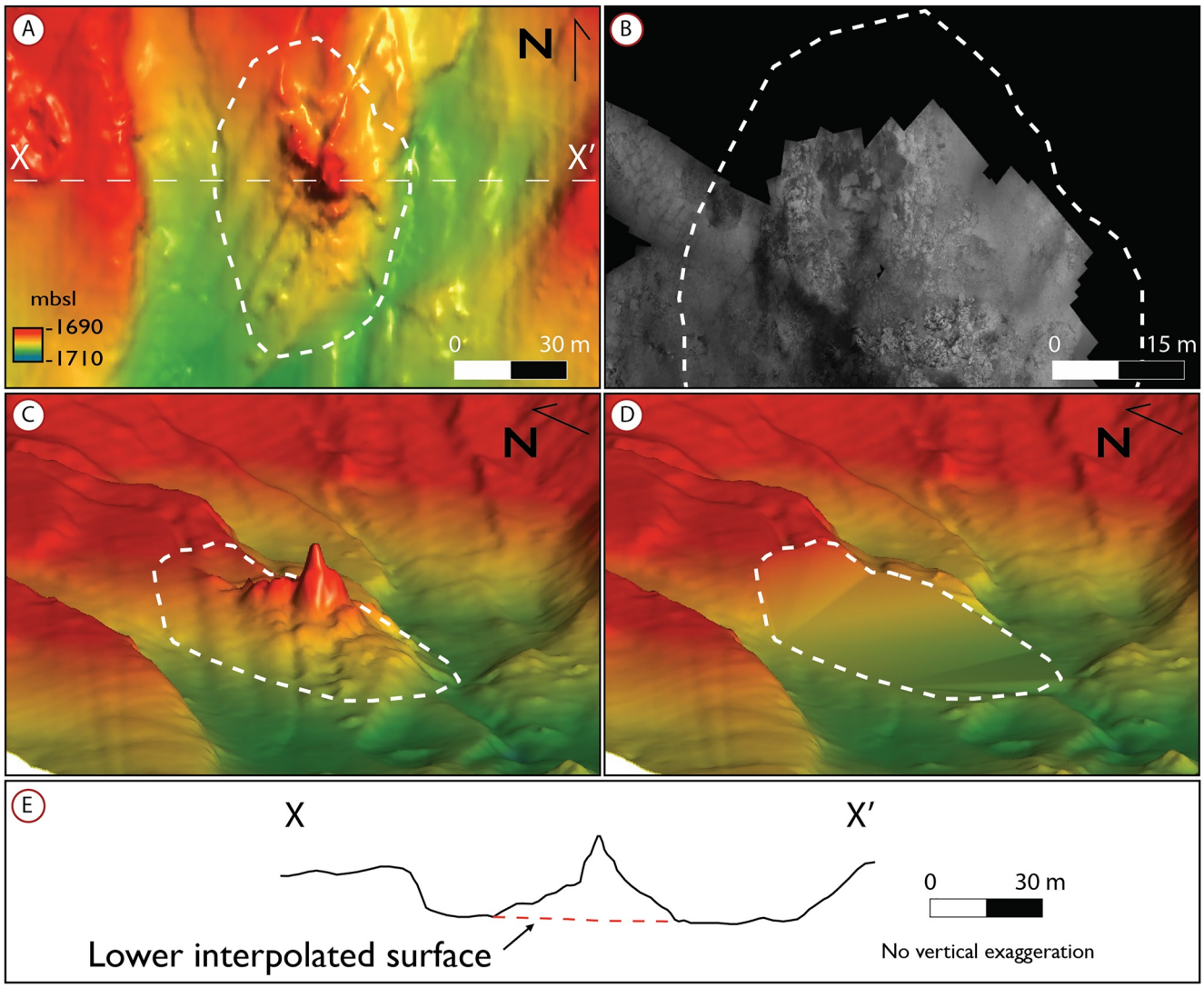

Figure 2. Volume calculations of hydrothermal deposits, illustrated using the Tour Eiffel site as an example. (a) Plan view of the of the bathymetry surrounding the Tour Eiffel site. White dashed outline shows the extent of the hydrothermal deposit, based on bathymetric features and visual confirmation from photomosaics of the seafloor. (b) Photomosaic coverage of Tour Eiffel site (*Bathyluck'09* photomosaic). (c) Oblique view of Tour Eiffel site with the dashed white line outlining the extent of the hydrothermal deposit used to define the lower boundary from which volumes were estimated. (d) Same view as (c) but with the bathymetry cropped and replaced by the interpolated lower boundary cut-off surface. (e) Cross-section X-X' from (a) showing a profile of the Tour Eiffel site including the lower interpolated surface (red dashed line) that results in a 10% uncertainty for the volume estimate.

additional samples were collected from precipitates that formed on temperature probes that were deployed in 2009 and 2012 and each recovered 1 year later from two active high temperature vents within the vent field (see zero age data in Table 1).

In addition to use of ^{226}Ra/Ba, detectable ^{228}Ra (half-life of 5.75 years) and ^{228}Th (half-life of 1.91 years) activities indicate the presence of relatively young barite in a sample (Ditchburn & de Ronde, 2017). Using the ^{228}Ra/^{226}Ra activity ratios, barite with ages from 3 to 35 years can be dated, and using the ^{228}Th/^{228}Ra activity ratio, barite younger than 12 years can be dated. Previous work, mainly at volcanic arcs, has shown that older hydrothermal barite can be incorporated into younger samples, thus affecting the overall sample age (de Ronde et al., 2014; Ditchburn & de Ronde, 2017). When these different isotope chronometers are applied to individual samples, the different calculated ages can be used to evaluate the degree of mixing and ages of different generations of barite.

Barium concentrations within the bulk samples were determined by instrumental neutron activation analysis at Activation Laboratories (Ancaster, Ontario, Canada). The accuracy and precision of Ba is better than ±5%, based

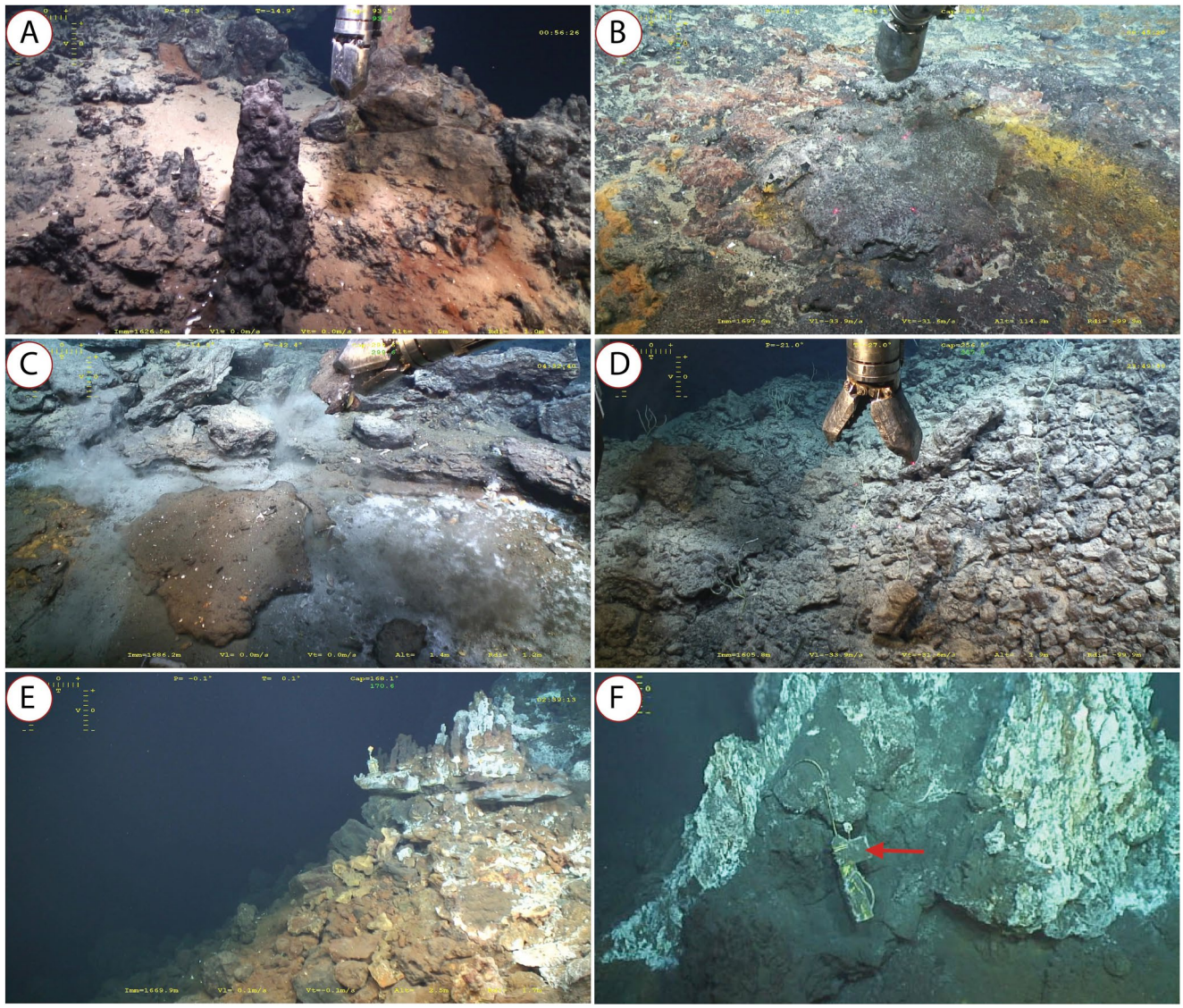

Figure 3. Hydrothermal deposit sample types. (a) Massive sulfide/sulfate chimney at the base of the Sintra site (sample MOM11-452-ROC1), which has an age of 6,647 ± 154 years (i.e., the oldest dated sample at Lucky Strike). (b) Hydrothermally cemented volcaniclastic breccia near Isabel (sample MOM15-607-ROC7), which has an age of 6,347 ± 154 years. (c) Hydrothermally cemented volcaniclastic breccia sampled 70 m W of Tour Eiffel (sample MOM15-607-ROC1), which has an age of 4,060 ± 157 years. (d) Hydrothermally cemented volcaniclastic breccia located 150 m NW from Bairro Alto (sample MOM15-605-ROC1), which has an age of 6,403 ± 517 years. (e) Massive sulfide/sulfate talus at the base of the Capelinhos site (sample MOM13-528-ROC1-S), which has an age of 817 ± 151 years. (f) Zero age sample, collected as hydrothermal precipitates that formed on a temperature probe (red arrow) at Crystal vent.

on repeat (n = 7) analysis of the GXR-1 standard. Radium-226, ^{228}Ra, and ^{228}Th activities of powdered samples was measured using a Canberra gamma spectrometer with a high-purity Germanium well-type detector with a counting time of 24 hr per sample. Raw spectra were converted to isotope activities using the ScienTissiMe software package by ScienTissiMe Inc. The initial N_0 value (1,053 ± 43 Bq/kg·wt%) was determined from the slope of the ^{226}Ra activity (Bq/kg) versus Ba (wt%) plot of the two zero-age samples. The age uncertainties were calculated using error propagation of all variables within the age equation.

3.2. Tonnage Estimate

The extent of hydrothermal chimneys and mounds on the seafloor were digitized from ~1 m resolution bathymetry (Figure 2a) collected during the MOMARETO cruise in 2006 and complemented with MOMAR'08 and Bathyluck'09 surveys, derived from ROV Victor 6000 and AUV Aster-X surveys (Escartín et al., 2015, 2021;

Table 1
^{226}Ra, ^{228}Ra, and ^{228}Th Activities and Ba Concentrations for Hydrothermal Sulfide/Sulfate Samples From Lucky Strike. Table S1 With Sample Coordinates and International Geo Sample Number (IGSN) Can be Found in Supporting Information

Sample	Ba (wt.%)	^{226}Ra activity (Bq/kg)	^{228}Ra activity (Bq/kg)	^{228}Th activity (Bq/kg)	$^{226}Ra/Ba$ age (years)	$^{228}Ra/^{226}Ra$ age (years)	$^{228}Th/^{228}Ra$ age (years)	Group	Sample type	Description
Y3										
MOM11-454-ROC7	1.93	2,083 ± 66	392 ± 19	181 ± 7	<500	26 ± 0.5	1.5 ± 0.2	IV	Massive sulfate/sulfide rock	Base of small active chimney
White Castle										
MOM15-603-ROC5	0.50	665 ± 21	75 ± 6	38 ± 2	<500	30 ± 0.7	1.7 ± 0.3	IV	Massive sulfate/sulfide rock	Block from active edifice
MOM15-603-ROC6	3.83	3,764 ± 119			<500	>35	>12	III	Massive sulfate/sulfide rock	Block from active edifice
Off axial graben to the W										
MOM15-605-ROC2	44.4	33,790 ± 1,502			749 ± 140	>35	>12	I	Massive sulfate/sulfide rock	From inactive site
Tour Eiffel										
MOM11-452-ROC4	0.50	99 ± 4			3,840 ± 274	>35	>12	I	Hydrothermally cemented volcaniclastic breccia	At the SE base of Tour Eiffel
MOM11-457-ROC8	3.45	2,730 ± 86	240 ± 13	115 ± 4	658 ± 125	32 ± 0.5	1.6 ± 0.2	II	Massive sulfate/sulfide rock	Small inactive chimney W of Tour Eiffel
MOM14-579-ROC1	2.38	2,085 ± 66	122 ± 8	56 ± 3	<500	36 ± 0.6	1.5 ± 0.2	IV	Massive sulfate/sulfide rock	Small inactive chimney, two barite generations
MOM13-532-ROC1	9.94	10,055 ± 316			<500	>35	>12	III	Massive sulfate/sulfide rock	Block in the E slope of Tour Eiffel
Site 85 m SW of Tour Eiffel										
MOM12-504-ROC1	11.2	4,715 ± 148			2,115 ± 120	>35	>12	I	Hydrothermally cemented volcaniclastic breccia	Block in inactive area 85 m SW of Tour Eiffel
Sintra										
MOM12-502-ROC1	38.1	31,140 ± 978	5,081 ± 227	2,356 ± 76	584 ± 120	27 ± 0.5	1.5 ± 0.2	II	Massive sulfate/sulfide rock	Active chimney
MOM11-452-ROC1	1.42	84 ± 3			6647 ± 154	>35	>12	I	Massive sulfate/sulfide rock	Small inactive chimney on sulfide-rich basement at the base of Sintra
Site 70 m W of Tour Eiffel (Chimiste)										
MOM15-607-ROC1	1.24	225 ± 8			4,060 ± 157	>35	>12	I	Hydrothermally cemented volcaniclastic breccia	Fragment next to inactive site 70 m W of Tour Eiffel
Between Isabel and Flores										

Table 1
Continued

Sample	Ba (wt.%)	^{226}Ra activity (Bq/kg)	^{228}Ra activity (Bq/kg)	^{228}Th activity (Bq/kg)	^{226}Ra/Ba age (years)	^{228}Ra/^{226}Ra age (years)	^{228}Th/^{228}Ra age (years)	Group	Sample type	Description
MOM15-607-ROC7	1.58	106 ± 4			6347 ± 154	>35	>12	I	Hydrothermally cemented volcaniclastic breccia	20 m SE from Isabel
MOM15-607-ROC6	0.27	88 ± 4			2,662 ± 466	>35	>12	I	Hydrothermally cemented volcaniclastic breccia	Southern base of the active site Flores
Site 150 m NW from Bairro Alto										
MOM15-605-ROC1	0.28	18 ± 2			6403 ± 517	>35	>12	I	Hydrothermally cemented volcaniclastic breccia	From inactive site
Capelinhos										
MOM14-583-ROC1-S	4.52	4,506 ± 142	266 ± 15	119 ± 5	<500	36 ± 0.6	1.5 ± 0.2	IV	Massive sulfate/sulfide rock	Block from the base of Capelinhos edifice, active high-T vents near, two barite generations
MOM13-528-ROC1-S	1.29	953 ± 30	140 ± 8	62 ± 3	817 ± 151	28 ± 0.6	1.5 ± 0.2	II	Massive sulfate/sulfide rock	Block from the base of Capelinhos edifice, active high-T vents near, two barite generations
Zero age										
LS-BS-WHOI (Y3)	3.23	3,369 ± 106	791 ± 37	333 ± 11	-	24 ± 13	1.4 ± 0.2	IV	Sample recovered from temperature probe	
HT010-CR12 (Crystal)	0.74	750 ± 24	177 ± 10	75 ± 3	-	24 ± 11	1.4 ± 0.2	IV	Sample recovered from temperature probe	

Note. Blank spaces indicate that activities were below the detection limit.

Ondréas et al., 2009). The extent of these hydrothermal deposits was also validated using ROV video imagery and a photomosaic data set (e.g., Figure 2b; Barreyre et al., 2012). Deposit volumes were calculated using Leapfrog Geo 4.3 software. These estimates are limited to hydrothermal material that has accumulated above the seafloor using an interpolated lower surface to represent the assumed geometry of the seafloor prior to hydrothermal deposition (Figures 2c–2e). An uncertainty of 10% is assigned to volume estimates. This uncertainty is derived from the resolution limitations of the bathymetric data and errors associated with defining the areal extent of the hydrothermal deposits in regions where photomosaics were not available. Evidence from VMS deposits studied on land (Galley et al., 2007) and from deep sea drilling (e.g., the active mound at TAG; Hannington et al., 1998), show that subseafloor replacement-style hydrothermal mineralization commonly occurs (e.g., Doyle

& Allen, 2003; Piercey, 2015). However, in this study we only consider the surficial hydrothermal material, and, as a result, our calculations provide minimum estimates for total accumulated hydrothermal material at Lucky Strike if subseafloor mineralization was also included.

To convert volumes to tonnages, a density for the hydrothermal deposits must be determined. An average density of 3.7 t/m^3 (range of 2.5–4.6 t/m^3 for individual samples) was determined for seafloor sulfide and sulfate rich samples from mid-ocean ridges and arc settings (Spagnoli et al., 2016). At the TAG active mound, Hannington et al. (1998) used an average density of 3.7 t/m^3 (range of 3.5–4 t/m^3) to calculate tonnage, while Graber et al. (2020) applied a density of 3.5 t/m^3 for the active mound. For an extensive study performed by Nautilus Minerals Inc., 415 hydrothermal deposit samples were analyzed for the resource estimate for the Solwara 1 hydrothermal deposit (Papua New Guinea), located in a backarc seting, and yielded an average density of 3.3 t/m^3 for sulfide-rich samples (Golder Associates Pty. Ltd., 2012). An average density of 3.1 t/m^3 was determined for the hydrothermal deposits at the Endeavor vent field (Juan de Fuca Ridge), and this value was used for a similar volume-tonnage estimate at that site (Jamieson et al., 2014; Tivey et al., 1999). For this study we use a value of 3.4 ± 0.3 t/m^3, which represents the average reported for mid-ocean ridge and arc settings and the value for the mineralogically similar Endeavor segment (Spagnoli et al., 2016; Tivey et al., 1999).

4. Results

4.1. Ages of Hydrothermal Deposits

Ages of hydrothermal samples from Lucky Strike, using the ^{226}Ra/Ba chronometer, range from zero (actively forming) to 6,647 ± 154 years (Table 1; Figure 4). The oldest sample was collected from the Sintra site, located on the eastern side of Lucky Strike (Figures 1 and 3a). This age overlaps within uncertainties of the next two oldest samples (6,403 ± 534 years and 6,347 ± 171 years) from the Bairro Alto site on the western side of Lucky Strike and the Chimiste site on the eastern side, respectively (Figure 1a). The oldest sample dated from Capelinhos has an age of 817 ± 187 years. Six of the 17 dated samples are hydrothermally cemented volcaniclastic breccias, that have also been previously described as "slabs" (Figures 3b–3d; Table 1; Humphris et al., 2002; Langmuir et al., 1997; Ondréas et al., 2009). These slabs are infilled by hydrothermal barite (0.27–11 wt.% Ba) and marcasite/pyrite, with the exception of MOM12-504-ROC1 that contains minor amounts of disseminated sphalerite and chalcopyrite. The age of these hydrothermal cements, which generally occur at the base of mound and chimney structures, are amongst the oldest hydrothermal precipitates in this study, and range from 6,403 ± 517 to 2,115 ± 120 years (Figure 4; Table 1). By contrast, chimney samples, with the exception of one sample from Sintra, yield younger ages that range from zero (active) to 817 years (Figures 3a–e3f). Therefore, the ages of the hydrothermal cements can provide a more confident estimate of the oldest ages for the vent field.

Nine samples have measurable ^{228}Ra and ^{228}Th activities, all from or near actively venting edifices (Table 1). The samples with no measurable ^{228}Ra and ^{228}Th activities are primarily from inactive regions from the vent field (including all of the volcaniclastic breccia, or "slab" samples), although three samples are from active vent sites. By combining the ^{226}Ra/Ba age data with the ^{228}Ra and ^{228}Th results, samples can be grouped into four categories (Table 1): Group I (n = 8) comprises the oldest samples dated (>~750 years) and contain no measurable ^{228}Ra or ^{228}Th; Group II (n = 3) consists of samples with ^{226}Ra/Ba ages of >500 years and measurable ^{228}Ra or ^{228}Th; Group III (n = 2) consists of samples with ^{226}Ra/Ba ages of <500 years and no measurable ^{228}Ra or ^{228}Th; Group IV (n = 6) consists of samples with ^{226}Ra/Ba ages of <500 years and measurable ^{228}Ra and ^{228}Th.

4.2. Deposit Size and Average Mass Accumulation Rate

Deposit size (reported as tonnage) and ages determined in this study are summarized in Figure 4. A total of 388,000 m^3, or 1.3 ± 0.2 Mt (converted using an average density of 3.4 ± 0.3 t/m^3) of hydrothermal material is estimated to have accumulated on the seafloor at Lucky Strike. at an average rate of 194 ± 28 t/yr, using the maximum age obtained in this study (6,647 years). The calculated overall accumulation rate should be considered a maximum rate because the maximum recorded age for the field (~6,650 years) represents the minimum duration of hydrothermal activity at this site.

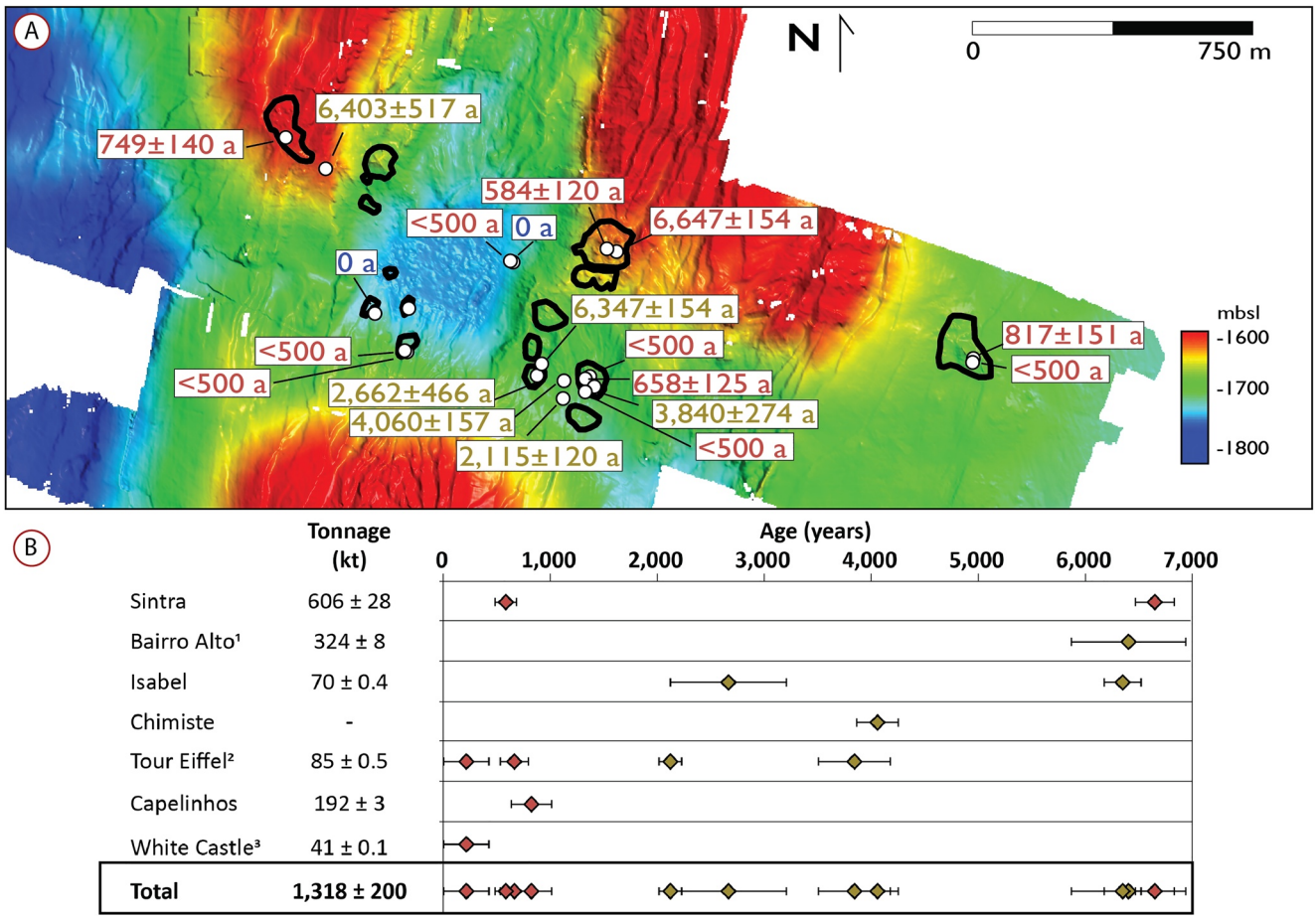

Figure 4. (a) Map of hydrothermal sites. Black outlines indicate areas where volumes of hydrothermal deposits have been determined. White circles indicate locations of samples dated using the ^{226}Ra/Ba method. The labeled ages in gold correspond to the hydrothermally cemented volcaniclastic rocks, red labels indicate sulfate/sulfide rocks, and blue labels indicate zero-age samples. (b) Tonnages, accumulation rates, and ages for sulfide/sulfate samples from different vent edifices at Lucky Strike. Red diamonds are sulfate/sulfide rock samples and gold diamonds correspond to hydrothermally cemented volcaniclastic samples. [1]Bairro Alto includes tonnage from three sites in the northwestern part of the area; [2]Tour Eiffel includes tonnages from Montsegur; [3]White Castle includes tonnages from four sites in the southwestern part of the area.

5. Discussion

5.1. Ages of Hydrothermal Vents

Hydrothermal venting, and therefore barite precipitation, has occurred throughout the lifespan of the hydrothermal system, either as continuous venting or at least continuous over prolonged episodes of active venting (e.g., 100–1000s of years; Figure 4b). Textural evidence such as barite crystal morphology and cross-cutting relationships for samples at Lucky Strike indicate a single generation of barite within most samples. However, three samples show evidence for at least two generations of barite (Table 1; Figure 5). Either way, the reported ^{226}Ra/Ba ages represent not necessarily a discrete age but, more likely, an average age of the barite in that sample. For example, a sample of chimney wall from an actively venting structure with an ^{226}Ra/Ba age of 600 years would contain a mixture of barite of ages that range from zero to >600 years. For this reason, all ages should be considered minimum ages.

The presence of barite with mixed ages at Lucky Strike is highlighted by comparing the ^{226}Ra/Ba ages with the ^{228}Ra and ^{228}Th data, as defined in the four sample groups (Table 1). Group I samples are older than ~500 years and have no measurable ^{228}Ra and ^{228}Th, indicating that these samples contain no barite younger than ~35 years old but likely contain a mixture of older barite. The absence of young barite within Group I samples is consistent with these samples being generally the oldest samples and collected from inactive regions of the vent field. Group II samples, which were collected from hydrothermally active areas of the vent field, are also

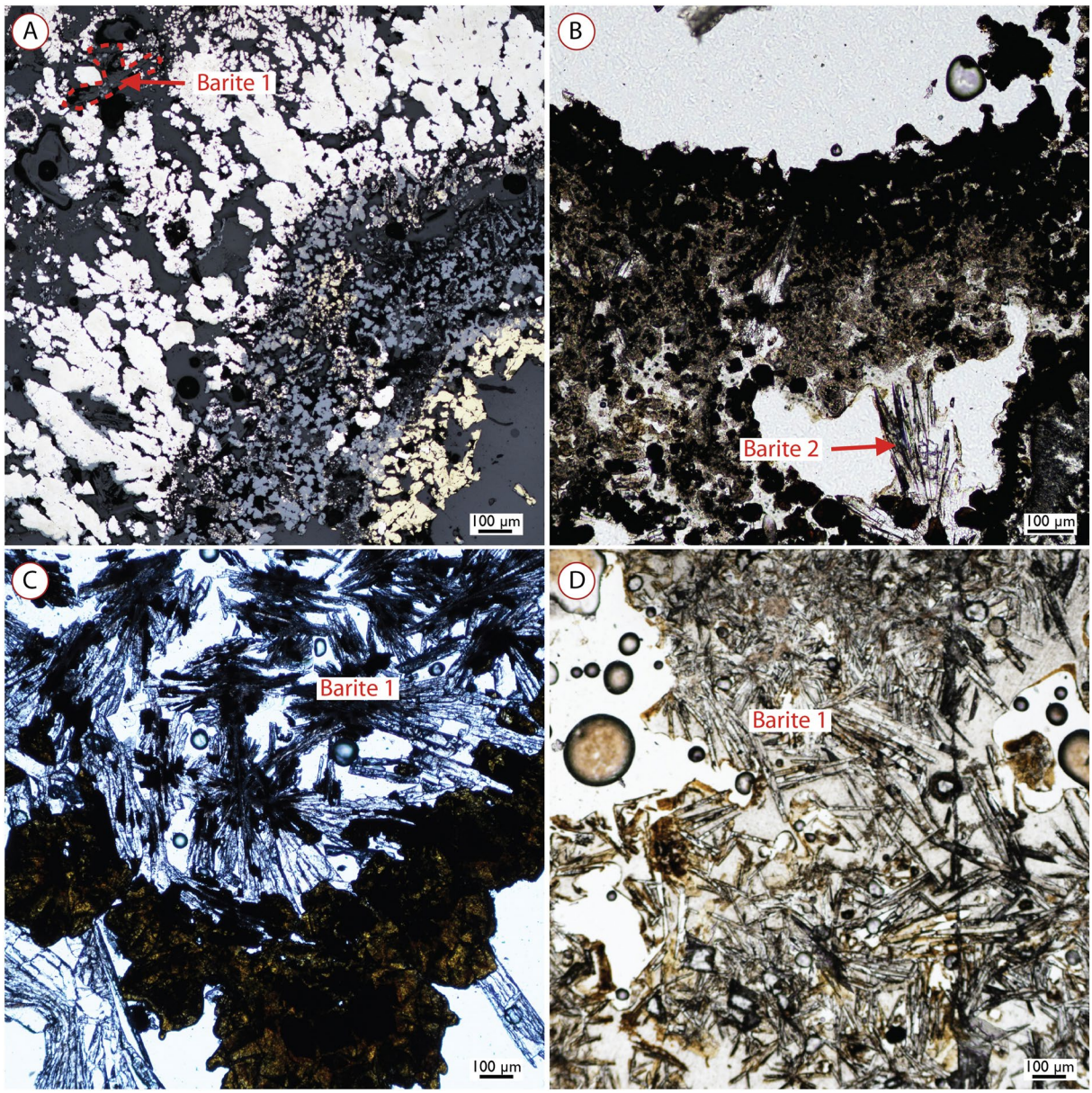

Figure 5. (a) Photomicrograph of a sample from the Tour Eiffel site (MOM14-579-ROC1) showing a generation of barite that has intergrown with marcasite (early stage). (b) Image from the same sample as A but in another area that shows a second generation of barite that has grown infilling vent conduits (late stage). (c) Single generation of barite from the Sintra site (MOM12-502-ROC1). (d) Single generation of barite at a site located west of the axial graben. Image A is a plane-polarized reflected light photomicrograph. Images B, C, D, are plane-polarized transmitted light photomicrographs.

older than ~500 years but, unlike Group I samples, do contain measurable ^{228}Ra and ^{228}Th, indicating barite in these samples that ranges in age from recently precipitated (<~12 years, based on ^{228}Th activity) to older than the reported ^{226}Ra/Ba age for each sample. Group III samples are younger than ~500 years and contain no measurable ^{228}Ra and ^{228}Th activities, which indicates absence of younger barite (<~35 years, based on ^{228}Ra activity). The combination of young ages but lack of recent barite is consistent with these samples being collected from inactive areas of otherwise actively venting edifices (Table 1). Group IV consists of samples younger than ~500 years with measurable ^{228}Ra and ^{228}Th activities, which is consistent with these samples being collected from active vents.

A plot of ^{228}Ra/Ba versus ^{226}Ra/Ba for samples that contain measurable ^{228}Ra activity can be used to determine if chimney barite contains a component of older remobilized barite from deeper in the system (de Ronde

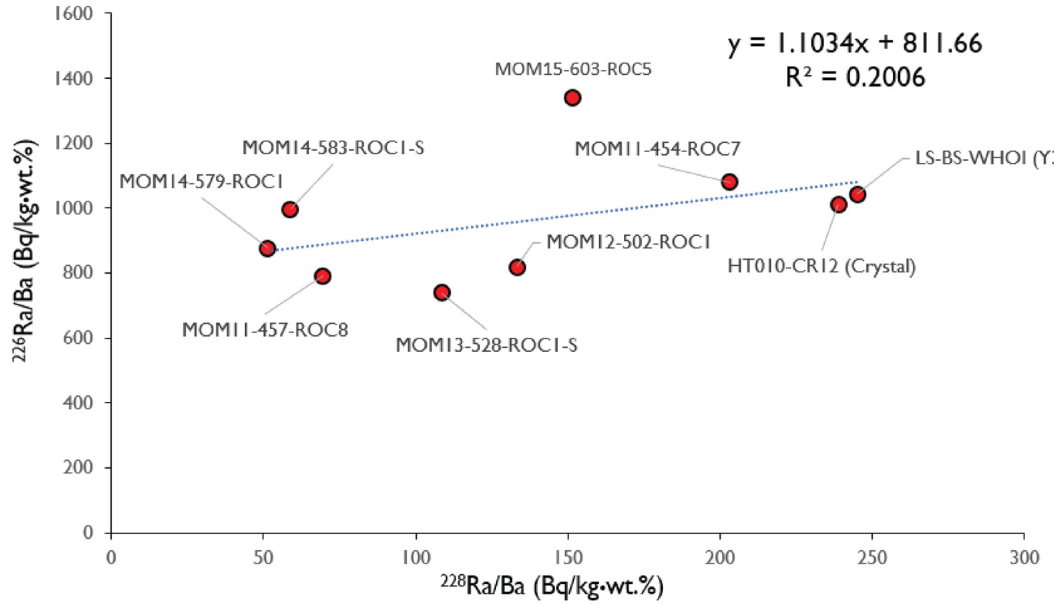

Figure 6. ^{228}Ra/Ba versus ^{226}Ra/Ba plot showing a mixing line of new and older barite in hydrothermal samples from the Lucky Strike vent field.

et al., 2014). A source of old barite with a defined age will result in a mixing line with a *y*-intercept that defines the ^{226}Ra/Ba ratio, and therefore the age, of the old barite. A ^{228}Ra/Ba versus ^{226}Ra/Ba plot for young samples at Lucky Strike does not result in a linear array, indicating that there is no discrete reservoir of old remobilized barite with a well defined age (Figure 6). Instead, a lack of defined linear array is consistent with samples containing barite representing a continuum of mixed ages.

5.2. Age and Evolution of the Lucky Strike Vent Field

The results of the barite dating indicate that there has been hydrothermal activity at Lucky Strike for at least ~6,600 years. The ages determined thus far (n = 17) show some age time gaps between ~6,000 and 4,000 years and ~2,000 and 800 years (Figure 4b). These age gaps could be interpreted to indicate that venting at Lucky Strike is episodic, as proposed for other sites on the MAR (Cherkashov et al., 2017; Lalou et al., 1995). If so, it is estimated that active hydrothermal venting has occurred for only ~3,400 years, or ~50% of the minimum age of the vent field. However, it is also possible that these age gaps simply reflect the limited number of dated samples. More sampling and dating would be required to resolve if the hydrothermal system at Lucky Strike has been continuous or discontinuous.

The results show that Lucky Strike is one of the youngest known basalt-hosted vent fields along the northern MAR. The youngest known basalt-hosted vent field along the MAR is Snake Pit (i.e., 3.7 ka; Lalou et al., 1990, 1993), and the next youngest, after Lucky Strike, is Puy des Folles (18 ka; Cherkashov et al., 2017). The common characteristic of these relatively youngdeposits is that they are located directly on the ridge axis, and are associated with volcanic edifices. By comparison, the oldest known basalt-hosted hydrothermal deposits along the MAR are 223 ka, from the Peterburgskoye field, which is located 16 km off axis, and the 119 ka Krasnov site, located 8 km from the ridge axis (Cherkashov et al., 2017). The average age of dated samples from the MAR is ~66 ka (Cherkashov et al., 2017).

The rifting event that has resulted in the dismemberment of the two volcanic edifices that host the Lucky Strike hydrothermal deposits is estimated to have initiated at ~60 ka, an age based on spreading rate and distances to the ridge axis and is therefore poorly constrained (Escartín et al., 2014). The fossil lava lake located between the rifted volcanic edifices shows no evidence of rifting and therefore represents the most recent volcanic event in this part of the segment (Humphris et al., 2002; Ondréas et al., 2009). The young ages of the hydrothermal deposits relative to the age of rifting and the spatial association of the venting with the recent fossil lava lake,

suggest that the initiation of the hydrothermal system feeding the vent field is related to the recent volcanic event that formed the lava lake. The occurrence of hydrothermal deposits surrounding the perimeter of the fossil lava lake suggests that older deposits may have been covered by recent volcanism (e.g., Humphris et al., 2002; Ondréas et al., 2009) and that any record of hydrothermal activity that would predate the recent volcanism has been obliterated.

The oldest known hydrothermal activity at Lucky Strike is recorded both at sites of significant sulfide/sulfate accumulation such as from the base of the Sintra site, and in hydrothermally cemented volcaniclastic breccias away from major hydrothermal edifices where there is no significant accumulation of hydrothermal material on the seafloor. Similar silificied and barite breccias have been described at the Clark Volcano, Kermadec arc, northeast of New Zealand (de Ronde et al., 2014). We suggest therefore, that early hydrothermal venting was likely widespread, and evolved to more focused and prolonged fluid flow that resulted in, and continues to form, the sulfide/sulfate mounds and chimney structures. The evolution of hydrothermal venting at Lucky Strike suggests that, for similar investigations of the age and evolution of other hydrothermal vent fields, hydrothermally cemented breccias (if present) may represent the oldest record of hydrothermal venting and should be targeted to provide greater insight into the maximum age of hydrothermal venting within the vent field.

5.3. Average Hydrothermal Mass Accumulation Rates

The calculated minimum average mass accumulation rate of 194 ± 28 t/yr for Lucky Strike is comparable to other reported mass accumulation rates for seafloor hydrothermal sites, which range from less than 100–~800 t/yr (Jamieson et al., 2014 and references therein). However, with the exception of TAG and Endeavor, these calculated rates rely primarily on rough visual estimates of deposit size, as opposed to more precise high-resolution (<2 m) bathymetry used in this study. High-temperature hydrothermal activity at the active mound at TAG began ~50,000 years ago, but may have experienced only ~5,000–10,000 years of active venting over that time (Lalou et al., 1995). Any episodicity of hydrothermal venting will decrease the average accumulation rate over the lifespan of a hydrothermal system. As a result, the mass accumulation rate for the active mound at TAG is 54 t/yr when considering the average rate over the lifespan of the mound, but is 360 t/yr when considering only periods of active venting (Jamieson et al., 2014). For Lucky Strike, although there are significant age gaps between samples (e.g., between 4,000 and 6,000 years; Figure 4b), the low number of samples dated can not resolve if hydrothermal activity has been episodic or continuous. The average accumulation rate of 194 ± 28 t/yr at Lucky Strike is therefore half of the rate at which the active mound at TAG accumulated during periods of activity. However, if an episodic scenario is assumed, the discontinuous accumulation rate over ~3,400 years of effective activity would be ~350 ± 95 t/yr, which is nearly identical to the rate calculated for TAG.

The scale of observation may have a significant influence when comparing mass accumulation rates between different vent fields. The overall areal extent of vent fields can vary significantly. For example, Lucky Strike and Endeavor have a similar estimated tonnage of 1.2–1.3 Mt (Jamieson et al., 2014); however, the higher accumulation rate of 400 t/yr along the Endeavor segment reflects high fluid fluxes associated with the large size of the vent field, which is distributed over ~60 km^2 of seafloor, compared to the Lucky Strike where vents cluster over an area of <2.5 km^2 (Jamieson et al., 2014). At both sites, venting generally occurs directly above the underlying axial magma chamber (with the exception of Capelinhos at Lucky Strike). At Lucky Strike, the axial magma chamber is thought to be located ~3 km below the seafloor and extends ~7 km along axis (Singh et al., 2006). In contrast, the magma chamber at Endeavor, while 2–3 km deep, extends up to 24 km along axis (Van Ark et al., 2007), thus covering a much longer ridge section that hosts active hydrothermal venting. It is therefore important to consider the size of the vent field when comparing accumulation rates between different fields.

Total hydrothermal fluid flux at Lucky Strike is estimated to range from 5.7 to 32 kg/s, based on heat flux measurements and the partitioning of high temperature focused fluid flow and lower temperature diffuse flow constrained using the seafloor photomosaic imagery (Barreyre, 2013; Barreyre et al., 2012). This flux range, combined with average vent fluid concentrations from Charlou et al. (2000) for the primary mineral forming elements (i.e., Cu, Zn, Fe, Si, Mn, S, Ba, Sr, and Ca), results in a dissolved hydrothermal mass flux to the seafloor of 352–1,966 t/yr, which is significantly higher than the average mass accumulation rate. This difference can be largely attributed to the venting and dispersal of a proportion of the dissolved mass flux in hydrothermal plumes discharging into the overlying water column (e.g., Elderfield & Schultz, 1996; German & Angel, 1995; Von Damm, 1990). The proportion of dissolved hydrothermal mass flux retained in the chimneys and mounds at the

seafloor, or "depositional efficiency" at Lucky Strike field is thus estimated to be between 9% and 51%. This range of values is similar to, or higher than other percent efficiency estimates, such as 5% for the Endeavor Field (Jamieson et al., 2014) and 30% for TAG (Humphris & Cann, 2000).

Overall, considering only accumulation during periods of hydrothermal activity, differences in accumulation rates at different vent fields result from differences in hydrothermal fluid flux (which may or may not correlate with vent field size), the efficiency of mineral precipitation, and the proportion of minerals that precipitate on the subseafloor. If these variables are considered individually, higher fluid fluxes will increase the rate of mineral precipitation, and higher degrees of mixing between ascending hydrothermal fluids and local seawater prior to venting will cause increased mineral precipitation within the deposit (and hence a lower proportion of metals lost to plumes) and a higher mass accumulation rate.

5.4. Implications for the Formation of VMS Deposits

This study focuses on the accumulation of hydrothermal material at the seafloor, and therefore quantifiable in terms of volume/tonnage using bathymetric data. However, significant hydrothermal mineralization can also occur within the immediate subsurface below hydrothermal vents, and ancient VMS deposits are frequently interpreted to comprise sulfide mineralization that accumulated both at the seafloor and as replacement below the seafloor (e.g., Franklin et al., 2005; Galley et al., 2007; Piercey, 2015), and therefore deposit mass accumulation becomes decoupled from volume accumulation at the seafloor. As a result, the rates of formation calculated for hydrothermal deposits on the seafloor using the methods described here cannot be directly compared to rates of formation of VMS deposits that likely include a component of subseafloor replacement mineralization. Instead, the seafloor rates represent minimum estimates for total seafloor and subseafloor mineralization. The application of drilling and or geophysical methods would be necessary to include the subseafloor component of any rate and tonnage calculations (Galley et al., 2021; Murton et al., 2019).

The degree of subsurface mineral precipitation is controlled largely by the porosity and permeability of the immediate substrate through which fluid flow occurs. At TAG, Graber et al. (2020) estimated an additional 30% of sulfide material in the subseafloor, based on drilling observations at the active mound at TAG (Hannington et al., 1998). However, using seismic surveys at TAG, Murton et al. (2019) suggested that subseafloor deposits can range from 2 to 5 times the amount that is above the seafloor as mounds and chimneys. Drilling at sediment-hosted Middle Valley resulted in an estimate of at least the same amount of sulfide material in the subsurface compared to the mound material above the seafloor (Zierenberg et al., 1998). However, sediment-hosted deposits represent an extreme endmember of subseafloor mineralization due to the high porosity of the substrate. Another consideration for Lucky Strike is the possibility of unaccounted hydrothermal accumulation at the seafloor that was buried under the fossil lava lake. In summary, for Lucky Strike the calculated volume-based rate of accumulation should be considered as a minimum mass accumulation rate when considering the additional inclusion of subseafloor mineralization. Nevertheless, if we consider a scenario similar to TAG, where the mass of subsurface hydrothermal material is up to five times the amount that occurs at the surface, then the total mass accumulation rate for Lucky Strike would be 900 t/yr, which is still comparable to other sites on the seafloor (Graber et al., 2020; Jamieson et al., 2014).

Accumulation rates have been estimated for some ancient VMS deposits, where the duration of ore formation is constrained by measured ages of volcanic rocks stratigraphically above and below the hydrothermal deposits, and deposit tonnages include deposition both above and below the seafloor. Using these constraints, the Archean Kidd Creek deposit in Ontario, Canada, formed at a minimum rate of ∼170 t/yr (Bleeker & Parrish, 1996; Bleeker & van Breemen, 2011; Hannington et al., 2017). Similarly, calculated accumulation rates for deposits within the Devonian-Mississippian Finlayson Lake VMS district in the Yukon Territory, Canada, include 75–800 t/yr for the Kudz Ze Kayah deposit, ∼8 t/yr for the GP4F deposit, and 40–200 t/yr for the Wolverine deposit (Manor et al., 2022). Therefore, although the lack of subseafloor data prevents direct comparisons between the modern seafloor and ancient deposits, the estimated accumulation rates from VMS deposits are comparable (within the same order of magnitude) to rates from the modern seafloor hydrothermal deposits. Based on the minimum accumulation rate estimated in this study (∼194 t/yr), the average mafic-dominated VMS deposit (∼4.8 Mt; Mosier et al., 2009) can form in under 25,000 years.

6. Conclusions

Results from ^{226}Ra/Ba dating of hydrothermal deposits within the Lucky Strike vent field indicate that the vent field is at least 6,600 years old, which is relatively young compared to other dated deposits along the MAR. Combined ^{226}Ra, ^{228}Ra, and ^{228}Th activities indicate that the ^{226}Ra/Ba ages represent average barite ages within each sample. Based on the number and distribution of sample ages, whether hydrothermal venting has been continuous or episodic remains unresolved. The relatively young age of the vent field is consistent with the hydrothermal field being located on a volcanically active ridge axis, where recent volcanism may have buried older deposits. The generally older age of the hydrothermally cemented volcaniclastic breccias suggests an initial stage of widespread hydrothermal activity that later evolved into more focused fluid flow at discrete sites that are represented by the major mound deposits.

A minimum of 1.3 Mt of hydrothermal material is estimated to have accumulated on the seafloor at Lucky Strike. This estimate does not account for hydrothermal sulfide-sulfate precipitation below the seafloor and thus should not be considered a resource estimate for this vent field. The calculated average mass accumulation rate at the seafloor is $\sim 194 \pm 28$ t/yr. If an episodic venting scenario is considered, the accumulation rate over the active periods would be $\sim 350 \pm 95$ t/yr. Although these accumulation rates are comparable to other sites along MORs, the Lucky Strike deposits notably occur within a relatively small seafloor footprint when compared to other well-characterized vent fields. The rates of accumulation at Lucky Strike along with other sites from the seafloor are similar to estimated rates of formation for some ancient volcanogenic massive sulfide deposits.

Data Availability Statement

All the geochronological and geochemical data is included in this paper and in the Supporting Information. The bathymetric data set can be accessed at https://www.seanoe.org/data/00694/80574/. To access data for samples using the IGSN go to https://www.geosamples.org/about/services.

Acknowledgments
This work was supported by the Canada Research Chair Program, an NSERC Discovery Grant, and RDC Leverage Grant to J.W. Jamieson.

References

Barreyre, T. (2013). *Dynamics and heat fluxes of the Lucky Strike hydrothermal field (mid-Atlantic Ridge, 37°17'N)*. Institut de Physique du Globe de Paris Université Paris Diderot.

Barreyre, T., Escartín, J., Garcia, R., Cannat, M., Mittelstaedt, E., & Prados, R. (2012). Structure, temporal evolution, and heat flux estimates from the Lucky Strike deep-sea hydrothermal field derived from seafloor image mosaics. *Geochemistry, Geophysics, Geosystems*, *13*(4), 1–29. https://doi.org/10.1029/2011GC003990

Bleeker, W., & Parrish, R. R. (1996). Stratigraphy and U-Pb zircon geochronology of Kidd Creek: Implications for the formation of giant volcanogenic massive sulphide deposits and the tectonic history of the Abitibi greenstone belt. *Canadian Journal of Earth Sciences*, *33*(8), 1213–1231. https://doi.org/10.1139/e96-092

Bleeker, W., & van Breemen, O. (2011). New geochronological, stratigraphic, and structural observations on the Kidd-Munro assemblage and the terrane architecture of the south-central Abitibi greenstone belt, Superior craton, Canada. In. *Results from the Targeted Geoscience Initiative III Kidd-Munro Project, Ontario Geological Survey*, *6258*, 142.

Bogdanov, Y. A., Lein, A. Y., Sagalevich, A. M., Ul'yanov, A. A., Dorofeev, S. A., & Ul'yanova, N. V. (2006). Hydrothermal sulfide deposits of the Lucky Strike vent field, mid-Atlantic Ridge. *Geochemistry International*, *44*(4), 403–418. https://doi.org/10.1134/S0016702906040070

Charlou, J. L., Donval, J. P., Douville, E., Jean-Baptiste, P., Radford-Knoery, J., Fouquet, Y., et al. (2000). Compared geochemical signatures and the evolution of menez gwen (35°50N) and Lucky Strike (37°17N) hydrothermal fluids, south of the Azores triple junction on the mid-Atlantic Ridge. *Chemical Geology*, *171*(1–2), 49–75. https://doi.org/10.1016/S0009-2541(00)00244-8

Cherkashov, G., Kuznetsov, V., Kuksa, K., Tabuns, E., Maksimov, F., & Beltenev, V. (2017). Sulfide geochronology along the northern equatorial mid-Atlantic Ridge. *Ore Geology Reviews*, *87*, 147–154. https://doi.org/10.1016/j.oregeorev.2016.10.015

de Ronde, C. E. J., Hannington, M. D., Stoffers, P., Wright, I. C., Ditchburn, R. G., Reyes, A. G., et al. (2005). Evolution of a submarine magmatic-hydrothermal system: Brothers volcano, southern Kermadec arc, New Zealand. *Economic Geology*, *100*(6), 1097–1133. https://doi.org/10.2113/gsecongeo.100.6.1097

de Ronde, C. E. J., Walker, S. L., Ditchburn, R. G., Tontini, F. C., Hannington, M. D., Merle, S. G., et al. (2014). The anatomy of a buried submarine hydrothermal system. *Clark Volcano*, *109*(8), 2261–2292. https://doi.org/10.2113/econgeo.109.8.2261

Ditchburn, R. G., & de Ronde, C. E. J. (2017). *Evidence for remobilization of barite affecting implications for the evolution of sea-floor volcanogenic massive sulfides*. *112*(5), 1231–1245. https://doi.org/10.5382/econgeo.2017.4508

Ditchburn, R. G., de Ronde, C. E. J., & Barry, B. J. (2012). Radiometric dating of volcanogenic massive sulfides and associated iron oxide crusts with an emphasis on 226Ra/Ba and 228Ra/226Ra in volcanic and hydrothermal processes at intraoceanic Arcs. *Economic Geology*, *107*(8), 1635–1648. https://doi.org/10.2113/econgeo.107.8.1635

Ditchburn, R. G., Graham, I. J., Barry, B. J., & de Ronde, C. E. J. (2004). Uranium series disequilibrium dating of black smoker chimneys. *New Zealand Science Review*, *61*, 54–56.

Doyle, M. G., & Allen, R. L. (2003). Subsea-floor replacement in volcanic-hosted massive sulfide deposits. *Ore Geology Reviews*, *23*(3–4), 183–222. https://doi.org/10.1016/S0169-1368(03)00035-0

Elderfield, H., & Schultz, A. (1996). Mid-Ocean Ridge hydrothermal fluxes and the chemical composition of the ocean. *Annual Review of Earth and Planetary Sciences*, *24*(1), 191–224. https://doi.org/10.1146/annurev.earth.24.1.191

Escartín, J., Barreyre, T., Cannat, M., Garcia, R., Gracias, N., Deschamps, A., et al. (2015). Hydrothermal activity along the slow-spreading Lucky Strike ridge segment (Mid-Atlantic Ridge): Distribution, heatflux, and geological controls. *Earth and Planetary Science Letters*, *431*, 173–185. https://doi.org/10.1016/j.epsl.2015.09.025

Escartín, J., Cannat, M., & Deschamps, A. (2021). Microbathymetry from AUV and ROV surveys (MOMARETO'06, MOMAR'08-leg1 and BATHYLUCK'09 cruises) along the Lucky Strike ridge segment (mid Atlantic Ridge). *SEANOE*. https://doi.org/10.17882/80574

Escartín, J., Soule, S. A., Cannat, M., Fornari, D. J., Düşünür, D., & Garcia, R. (2014). Lucky Strike seamount: Implications for the emplacement and rifting of segment-centered volcanoes at slow spreading mid-ocean ridges. *Geochemistry, Geophysics, Geosystems*, *15*(11), 4157–4179. https://doi.org/10.1002/2014GC005563.Received

Fouquet, Y., Ondréas, H., Charlou, J. L., Donval, J.-P., Radford-Knoery, J., Costa, I., et al. (1995). Atlantic lava lakes and hot vents. *Nature*, *377*(6546), 201. https://doi.org/10.1038/377201a0

Franklin, J. M., Gibson, H. L., Jonasson, I. R., & Galley, A. G. (2005). Volcanogenic massive sulfide deposits. *Economic Geology 100th Anniversary*, 523–560. https://doi.org/10.1016/B978-0-08-095975-7.01120-7

Galley, A. G., Hannington, M. D., & Jonasson, I. R. (2007). *Volcanogenic massive sulphide deposits*. Geological Association of Canada.

Galley, C., Lelièvre, P., Haroon, A., Graber, S., Jamieson, J. W., Szitkar, F., et al. (2021). Magnetic and gravity surface geometry inverse modelling of the TAG active mound. *Journal of Geophysical Research: Solid Earth*.

German, C. R., & Angel, M. V. (1995). Hydrothermal fluxes of metals to the oceans: A comparison with anthropogenic discharge. *Geological Society - Special Publications*, *87*(87), 365–372. https://doi.org/10.1144/GSL.SP.1995.087.01.28

Golder Associates Pty Ltd. (2012). *Mineral resource estimate, Solwara projet, bismarck sea*. PNG: Technical Report compiled under NI43-101.

Graber, S., Petersen, S., Yeo, I., Szitkar, F., Klischies, M., Jamieson, J. W., et al. (2020). Structural control, evolution, and accumulation rates of massive sulfides in the TAG hydrothermal field. *Geochemistry, Geophysics, Geosystems*, *21*(9). https://doi.org/10.1029/2020GC009185

Hannington, M. D. (2014). Volcanogenic massive sulfide deposits. *Treatise on Geochemistry*, *13*, 463–488. https://doi.org/10.1016/B978-0-08-095975-7.01120-7

Hannington, M. D., Galley, A. G., Herzig, P. M., Petersen, S., & Charles, K. (1998). Comparison of the TAG mound and stockwork complex with Cyprus-type massive sulfide deposits. *Proceedings of the Ocean Drilling Program, Scientific Results*, *158*, 389–415. https://doi.org/10.2973/odp.proc.sr.158.217.1998

Hannington, M. D., Gemmell, T., & Monecke, T. (2017). The Kidd Creek volcanogenic massive sulfide deposit—an update. In T. Monecke, P. Mercier-Langevin, & B. Dubé (Eds.), *Archean base and precious metal deposits, southern abitibi greenstone belt, Canada*, *Reviews in economic geology* (Vol. 19, pp. 81–102). https://doi.org/10.5382/Rev.19.03

Humphris, S. E., & Cann, J. R. (2000). Constraints on the energy and chemical balances of the modern TAG and ancient Cyprus seafloor sulfide deposits. *Journal of Geophysical Research*, *105*(B12), 28477–28488. https://doi.org/10.1029/2000jb900289

Humphris, S. E., Fornari, D. J., Scheirer, D. S., German, C. R., & Parson, L. M. (2002). Geotectonic setting of hydrothermal activity on the summit of Lucky Strike seamount (37°17'N, mid-Atlantic Ridge). *Geochemistry, Geophysics, Geosystems*, *3*(8), 1–24. https://doi.org/10.1029/2001GC000284

Jamieson, J. W., Clague, D. A., & Hannington, M. D. (2014). Hydrothermal sulfide accumulation along the eEndeavor segment , juan de Fuca ridge. *Earth and Planetary Science Letters*, *395*, 136–148. https://doi.org/10.1016/j.epsl.2014.03.035

Jamieson, J. W., Hannington, M. D., Clague, D. A., Kelley, D. S., Delaney, J. R., Holden, J. F., et al. (2013). Sulfide geochronology along the eEndeavor segment of the juan de Fuca ridge. *Geochemistry, Geophysics, Geosystems*, *14*(7), 2084–2099. https://doi.org/10.1002/ggge.20133

Lalou, C., & Brichet, E. (1982). Ages and implications of East Pacific Rise sulphide deposits 21°N. *Nature*, *300*(5888), 169–171. https://doi.org/10.1038/300169a0

Lalou, C., Reyss, J.-L., Brichet, E., Arnold, M., Thompson, G., Fouquet, Y., & Rona, A. (1993). New age data for mid-Atlantic Ridge hydrothermal sites: TAG and snakepit chronology revisited. *Journal of Geophysical Research*, *98*(B6), 9705–9713. https://doi.org/10.1029/92JB01898

Lalou, C., Reyss, J.-L., Brichet, E., Rona, P. A., & Thompson, G. (1995). Hydrothermal activity on a 10(5)-year scale at a slow-spreading ridge, TAG hydrothermal field, Mid-Atlantic Ridge 26°N. *Journal of Geophysical Research: Solid Earth*, *100*(B9), 17855–17862. https://doi.org/10.1029/95jb01858

Lalou, C., Thompson, G., Arnold, M., Brichet, E., Druffel, E., & Rona, P. A. (1990). Geochronology of TAG and snakepit hydrothermal fields, mid-Atlantic Ridge: Witness to a long and complex hydrothermal history. *Earth and Planetary Science Letters*, *97*(1–2), 113–128. https://doi.org/10.1016/0012-821x(90)90103-5

Langmuir, C., Humphris, S. E., Fornari, D., Van Dover, C., Von Damm, K., Tivey, M. K., et al. (1997). Hydrothermal vents near a mantle hot spot: The Lucky Strike vent field at 37°N on the mid-Atlantic Ridge. *Earth and Planetary Science Letters*, *148*(1–2), 69–91. https://doi.org/10.1016/S0012-821X(97)00027-7

Langmuir, C. H., Klinkhammer, G., Bougault, H., & Scientific Party, S. (1992). *FAZAR cruise report*. Palisades.

Lowell, R. P., Rona, P. A., & Von Herzen, R. P. (1995). Seafloor hydrothermal systems. *Journal of Geophysical Research*, *100*(10), 327–352. https://doi.org/10.1029/94jb02222

Manor, M. J., Piercey, S. J., Wall, C. J., & Denisová, N. (2022). High precision CA-ID-TIMS U-Pb zircon geochronology of felsic rocks in the Finlayson Lake VMS district, Yukon : Linking Paleozoic basin-scale accumulation rates to the occurrence of subseafloor replacement-style mineralization. *Economic Geology*.

Mittelstaedt, E., Escartín, J., Gracias, N., Olive, J., Barreyre, T., Davaille, A., et al. (2012). Quantifying diffuse and discrete venting at the Tour Eiffel vent site, Lucky Strike hydrothermal field. *Geochemistry, Geophysics, Geosystems*, *13*(4). https://doi.org/10.1029/2011GC003991

Mosier, B. D. L., Berger, V. I., & Singer, D. A. (2009). *Volcanogenic massive sulfide deposits of the world — database and grade and tonnage models*. https://doi.org/10.3133/ofr20091034

Münch, U., Lalou, C., Halbach, P., & Fujimoto, H. (2001). Relict hydrothermal events along the super-slow Southwest Indian spreading ridge near 63°56′E- Mineralogy, chemistry and chronology of sulfide samples. *Chemical Geology*, *177*(3–4), 341–349. https://doi.org/10.1016/S0009-2541(00)00418-6

Murton, B. J., Lehrmann, B., Dutrieux, A. M., Martins, S., de la Iglesia, A. G., Stobbs, I. J., et al. (2019). Geological fate of seafloor massive sulphides at the TAG hydrothermal field (Mid-Atlantic Ridge). *Ore Geology Reviews*, *107*(March), 903–925. https://doi.org/10.1016/j.oregeorev.2019.03.005

Ondréas, H., Cannat, M., Fouquet, Y., Normand, A., Sarradin, P. M., & Sarrazin, J. (2009). Recent volcanic events and the distribution of hydrothermal venting at the Lucky Strike hydrothermal field, Mid-Atlantic Ridge. *Geochemistry, Geophysics, Geosystems*, *10*(2). https://doi.org/10.1029/2008GC002171

Piercey, S. J. (2015). A semipermeable interface model for the Genesis of subseafloor replacement-type volcanogenic massive sulfide (VMS) deposits. *Economic Geology*, *110*(7), 1655–1660. https://doi.org/10.2113/econgeo.110.7.1655

Singh, S. C., Crawford, W. C., Carton, H., Seher, T., Combier, V., Cannat, M., et al. (2006). Discovery of a magma chamber and faults beneath a Mid-Atlantic Ridge hydrothermal field. *Nature*, *442*(7106), 1029–1032. https://doi.org/10.1038/nature05105

Spagnoli, G., Hannington, M., Bairlein, K., Hördt, A., Jegen, M., Petersen, S., & Laurila, T. (2016). Electrical properties of seafloor massive sulfides. *Geo-Marine Letters*, *36*(3), 235–245. https://doi.org/10.1007/s00367-016-0439-5

Tivey, M. K., Stakes, D. S., Cook, T. L., Hannington, M. D., & Petersen, S. (1999). A model for growth of steep-sided vent structures on the Endeavor Segment of the Juan de Fuca Ridge: Results of a petrologic and geochemical study. *Journal of Geophysical Research*, *104*(B10), 22859–22883. https://doi.org/10.1029/1999JB900107

Van Ark, E. M., Detrick, R. S., Canales, J. P., Carbotte, S. M., Harding, A. J., Kent, G. M., et al. (2007). Seismic structure of the Endeavor segment, Juan de Fuca Ridge: Correlations with seismicity and hydrothermal activity. *Journal of Geophysical Research*, *112*(2), 1–22. https://doi.org/10.1029/2005JB004210

Von Damm, K. L. (1990). Seafloor hydrothermal activity: Black smoker chemistry and chimneys. *Annual Review of Earth and Planetary Sciences*, *18*(1), 173–204. https://doi.org/10.1146/annurev.ea.18.050190.001133

Wang, Y., Han, X., Jin, X., Qiu, Z., Ma, Z., & Yang, H. (2012). Hydrothermal activity events at kairei field, central Indian ridge 25°S. *Resource Geology*, *62*(2), 208–214. https://doi.org/10.1111/j.1751-3928.2012.00189.x

Zierenberg, R. A., Fouquet, Y., Miller, D. J., Bahr, J. M., Baker, P. A., Bjerkgard, T., et al. (1998). The deep structure of a sea-floor hydrothermal deposit. *Nature*, *392*, 485–488. https://doi.org/10.1038/33126